Role of K-feldspar and quartz in global ice nucleation by mineral dust in mixed-phase clouds

Marios Chatziparaschos[1,2], Nikos Daskalakis[3], Stelios Myriokefalitakis[4], Nikos Kalivitis[1], Athanasios Nenes[2,7], María Gonçalves Ageitos[5,6], Montserrat Costa-Surós[5], Carlos Pérez García-Pando[5,10], Medea Zanoli[3], Mihalis Vrekoussis[3,8,9] and Maria Kanakidou[1,2,3]*

[1]Environmental Chemical Processes Laboratory (EPCL), Department of Chemistry, University of Crete, Heraklion
[2]Center for the Study of Air Quality and Climate Change (C-STACC), Institute of Chemical Engineering Sciences (ICE-HT), Foundation for Research and Technology, Hellas) (FORTH), Patras, Greece
[3]Laboratory for Modelling and Observation of the Earth System (LAMOS), Institute of Environmental Physics (IUP), University of Bremen, Bremen, Germany
[4]Institute for Environmental Research and Sustainable Development, National Observatory of Athens (NOA), GR-15236 Palea Penteli, Greece
[5]Barcelona Supercomputing Center (BSC), Barcelona, Spain
[6]Department of Project and Construction Engineering, Universitat Politècnica de Catalunya – Barcelona TECH (UPC), Barcelona, Spain
[7]Laboratory of Atmospheric Processes and their Impacts (LAPI), School of Architecture, Civil and Environmental Engineering (ENAC), Ecole Polytechnique Federale de Lausanne, Switzerland
[8]Center of Marine Environmental Sciences (MARUM), University of Bremen, Germany
[9]Climate and Atmosphere Research Center (CARE-C), The Cyprus Institute, Nicosia, Cyprus Laboratory of Atmospheric
[10]ICREA, Catalan Institution for Research and Advanced Studies, Barcelona, Spain

Correspondence to: Maria Kanakidou (mariak@uoc.gr)

Abstract. Ice Nucleating Particles (INPs) enable ice formation, profoundly affecting the microphysical and radiative properties, lifetimes, and precipitation rates of clouds. Mineral dust emitted from arid regions, particularly potassium-containing feldspar (K-feldspar), has been shown to be a very effective INP through immersion freezing in mixed-phase clouds. However, despite quartz has a significantly lower ice nucleation activity, it is more abundant than K-feldspar in atmospheric desert dust, and therefore may be a significant source of INP. In this contribution, we test this hypothesis by investigating the global and regional importance of quartz as a contributor to INP in the atmosphere relative to K-feldspar. We have extended a global 3-D chemistry transport model (TM4-ECPL) to predict INP concentrations from both K-feldspar and quartz mineral dust particles with state-of-the-art parameterizations using the ice nucleation active surface site approach for immersion freezing. Our results show that although K-feldspar remains the most important contributor to INP concentrations globally, affecting mid-level mixed-phase clouds, the contribution of quartz can also be significant. Quartz dominates the lowest and the highest altitudes of dust-derived INP, affecting mainly low-level and high-level mixed-phase clouds. The consideration of quartz INP also improves the comparison between simulations and observations at low temperatures. Our simulated INP concentrations predict ~51% of the observations gathered from different campaigns within an order of magnitude and ~69% within one and a half order of magnitude, despite the omission of other potentially important INP aerosol precursors like marine bioaerosols. Our findings support the inclusion of quartz in addition to K-feldspar as INP in climate models and highlight the need of further constraining their abundance in arid soil-surfaces along with their abundance, size distribution and mixing state in the emitted dust atmospheric particles.

1 Introduction

In the atmosphere, aerosol particles are emitted from various natural and anthropogenic sources or formed from precursor gases. Aerosols are important for climate due to their interactions with radiation, by scattering and absorbing light (direct climate effect) (Miller et al., 2014) and their ability to act as precursors of clouds, modulating clouds' global distribution and radiative forcing (indirect effect) (IPCC, 2021), along with the hydrological cycle (Seinfeld et al., 2016). The radiative

1

properties and microphysics of clouds are particularly sensitive to aerosol concentration, composition and size (Boucher, 2015). Aerosols serve as cloud condensation nuclei (CCN) to form liquid cloud droplets (Seinfeld et al., 2016) or as ice nucleating particles (INP) to form ice crystals (Murray et al., 2012). Ice formation in clouds proceeds for supersaturation relative humidity relative to ice (RHi) (Kanji et al., 2019) by both heterogeneous and homogeneous freezing at temperatures lower than −38°C (Liu et al., 2012) and by heterogeneous freezing at warmer temperatures (DeMott et al., 2010; Murray et al., 2012; O'Sullivan et al., 2016; Price et al., 2018). INP can dramatically reduce the lifetime of shallow clouds (Vergara-Temprado et al., 2018). Also, the presence of INP may alter the development of deep convective clouds through convective invigoration (Rosenfeld et al., 2008), where enhanced glaciation of clouds increases the release of latent heat and buoyancy, which in turn increases up-draught and vertical development, thus modifying the cloud structure (Lohmann and Gasparini, 2017).

In mixed-phased clouds (MPCs), adding CCN with low INP concentrations suppresses precipitation, and the supercooled clouds are mostly composed of liquid droplets especially in warm mixed-phase orographic clouds (Fan et al., 2017), so that CCN variations directly modulate the clouds' microphysical properties and radiative forcing (Vergara-Temprado et al., 2018). Increases in INP concentrations tend to glaciate clouds as water vapor preferentially partitions to ice owing to its lower equilibrium vapor pressure than water (Bergeron-Fiendesein process; Pruppacher et al., 1998). Given that INP tend to be orders of magnitude lower in concentration than CCN (Seinfeld et al., 2016), a cloud that glaciates can rapidly redistribute its water from many cloud droplets down to much fewer ice crystals, leading to the formation of precipitation (Pruppacher et al., 1998b; Seinfeld et al., 2016). This entails a shorter cloud lifetime, lower albedo, less reflected radiation, and thus less cooling of the atmosphere than by liquid clouds (DeMott et al., 2010). Secondary processes (ice-ice collisions, droplet riming and droplet shattering) can modulate further these phenomena (e.g., Georgakaki et al., 2022; Sotiropoulou et al., 2021; Field et al., 2016) so that ice production is promoted even at extremely low INP concentrations (e.g., Morales Betancourt et al., 2012; Sullivan et al., 2018). High concentrations of CCN can further modulate these processes by reducing the efficiency of riming and droplet shattering (e.g., Lance, 2012). Although global aerosol models consider the aerosol-cloud droplet link (Ghan et al., 2011), much work remains to improve the description of ice formation (e.g. Vergara-Temprado et al., 2018), since the dynamics and properties of mixed-phase clouds are among the largest uncertainties in climate models (Fan et al., 2016). Murray et al. (2021) suggest that in a warmer future climate, ice in mixed-phase clouds will be replaced by liquid water, potentially leading to strong negative feedback. However, it is uncertain whether clouds damp or amplify warming, and a key factor of this uncertainty is how models estimate the concentration of INP. Many thermodynamic and microphysical feedbacks determine the glaciation state and properties of mixed-phase clouds, all of which can be affected by perturbations in CCN and INP concentrations (Solomon et al., 2018). Representing mixed-phase cloud properties in models requires an accurate description of INP along with the dynamical drivers of ice and cloud droplet formation. To achieve this, parameterizations of ice-nucleating properties of the aerosol components, which are species-specific, need to be considered in climate models (Murray et al., 2012).

While several aerosol types, like bioaerosol, black carbon and dust, have been identified to act as INP, the most important INP in the global atmosphere is thought to be mineral dust emitted into the atmosphere from deserts and other arid and semi-arid regions (Murray et al., 2012; Seinfeld et al., 2016). This is supported by a plethora of observational and modelling studies; the most direct evidence perhaps is measurements showing that ice crystal residuals in mixed-phase clouds are strongly enhanced in mineral dust (Pratt et al., 2009). Initially, most ice nucleation studies focused on clay minerals (Hoose and Möhler, 2012; Roberts and Hallett, 1969). Clays tend to be hydrophilic and, therefore can act as a CCN, which is a prerequisite for acting as an immersion mode INP (Kumar et al., 2011), and are transported over longer distances from the source regions due to their higher abundance in the smallest dust sizes and hence longer lifetime (Ginoux, 2017; Kok et al., 2017). More recently, it was

2

shown that among dust minerals, alkali feldspar, in particular the potassium feldspar (K-feldspar), nucleate ice more efficiently than plagioclase (Ca-feldspar) (Harrison et al., 2016). Also Na-rich feldspar is very ice-active but was found to lose its ice-activity with time compared to K-feldspar (Harrison et al., 2016), thus, K-feldspar is the most efficient INP. Note, however, that little is known about the processes governing the IN capability of these minerals, so more work is needed to unravel their effect and contribution for all possible ice formation conditions (Burrows et al., 2022). To explain the enhanced K-feldspar ice activity, it has been suggested that surface -OH groups on feldspars exposed to surface defects i.e. steps, cracks, and cavities, are responsible for its high ice nucleation efficiency by allowing ice-like structures to form (Kiselev et al., 2017). However, other minerals in the airborne dust remain insufficiently characterized regarding their ice nucleating activity. Quartz is a major component of airborne mineral dust but has lower ice nucleation ability than K-feldspar, with approximately 2 orders of magnitude less active site density (Harrison et al., 2019). Several studies have shown that quartz can also be a significant source of INP (Kumar et al., 2019; Senthil Kumar and Rajkumar, 2013; Harrison et al., 2019). Boose et al. (2016) investigated the representativeness of surface-collected dust for the airborne dust particles and showed a correlation between the INP activity of nine desert dust types and the combined concentration of quartz and K-feldspar, emphasizing the importance of taking into account the presence of both quartz and K-feldspar in the atmosphere for INP modelling.

Several approaches have been proposed to parameterize INP in climate models (e.g. Lohmann and Diehl, 2006; Spracklen and Heald, 2014; Wang et al., 2014). The first empirical parameterizations to calculate heterogeneous ice nucleation assumed that INP concentrations depend on i) temperature only (Meyers et al., 1992) or ii) temperature and the concentration of aerosol particles with a diameter larger than 0.5 μm (DeMott et al., 2010). These parameterizations did not consider additional important complexities such as chemical composition variations over time and space. The simplest and most performant parameterization is based on the ice nucleating active surface sites concept (Vali et al., 2015). This approach adopts the so-called singular hypothesis that assumes that each droplet contains a single ice nucleating particle active in a given temperature interval and the time dependence (stochasticity) of nucleation is of secondary importance (Vali et al., 2015). This hypothesis allows formulating a very simple link between aerosol chemical composition (surface structure), size distribution and an ice nucleation spectrum constrained by experimental data (e.g., Barahona and Nenes, 2009), from which one can predict INP as a function of supersaturation (in the deposition mode) or temperature (in the immersion mode). Immersion freezing occurs when ice nucleation is initiated by an INP that becomes immersed in an aqueous solution or water droplet via activation of CCN during liquid cloud formation and it is thought to be the most dominant freezing mechanism for mixed-phase clouds (Kanji et al., 2017). This is the ice formation pathway we focus on in this study. Different materials are assumed to have a different ice active density (n_s) per surface unit and a critical temperature below which an INP with multiple nucleation sites activates in the immersion mode to form ice (Hoose et al., 2010; Murray et al., 2012). Only a few INP parameterizations for immersion freezing mode explicitly consider n_s, and only recently, models that adopt this level of compositional complexity have emerged, mainly considering one type of INP from the most active mineral K-feldspar (Atkinson et al., 2013; Vergara-Temprado et al., 2017).

Harrison et al. (2019) proposed a new parameterization based on experimental work in immersion freezing mode by testing 10 naturally occurring quartz samples that highlighted the variability in their ice-nucleating ability. It was observed that the quartz group of minerals is generally less active than K-feldspars, with the most active quartz samples being of similar activity to some K-feldspars. It was also found that the ice-nucleating activity of some quartz samples is very sensitive to ageing when exposed to air and water, contrary to other quartz and K-feldspars samples. This variability indicates that mineral dust particles do not nucleate ice through a lattice-matching mechanism. The latter is consistent with recent observations that ice nucleation occurs at active sites (Holden et al., 2019). However, once in the atmosphere, mineral dust particles undergo ageing through the condensation of sulfates, nitrates and secondary organic aerosol material, becoming soluble and thus promoting wet

3

scavenging (Abdelkader et al., 2017). The occurrence of such atmospheric ageing of INP via coating by acids or water-soluble organics that modifies the ice-nucleating efficiency of aerosols is supported by the detection of sulphate and/or nitrate peaks of the IN active particles using single particle analysis by micro-Raman spectroscopy (Iwata and Matsuki, 2018). In addition, the solution environment may substantially impact the ice nucleation efficiency of both quartz and feldspar (Whale et al., 2018; Kumar et al., 2019), but the study of the impact of this process on INP is beyond the scope of the present study.

Here we present, to our knowledge, the first global modelling study of the role of airborne mineral dust as a precursor of INP, accounting for both dust's quartz and feldspar contents. We simulate the three-dimensional global distribution of INP concentrations, evaluate the model results against observations, and investigate a) the importance of quartz relative to feldspar in INP formation and b) potentially missing INP sources other than dust minerals. To achieve this, we use a well-documented global 3-D chemistry-transport model to simulate the global temporally and spatially varying immersion-mode distributions of INP from feldspar and quartz minerals.

2 Methods

2.1 Global modelling

For the present study, we use the global 3-dimensional chemistry-transport model TM4-ECPL (Daskalakis et al., 2016, 2022; Myriokefalitakis et al., 2016, 2015; Kanakidou et al., 2020) driven by ERA-interim reanalysis meteorological fields produced with the European Centre for Medium-Range Weather Forecasts (ECMWF) meteorological model (Dee et al., 2011). The specific model version has a horizontal resolution of 3° longitude by 2° latitude with 25 hybrid pressure vertical levels from surface up to 0.1hPa (about 65 km) and uses a model time step of 30 minutes. The model simulates tropospheric chemistry accounting for non-methane volatile organics, all major aerosol components, including dust, and the atmospheric cycles of nitrogen, iron and phosphorus (Tsigaridis et al., 2014; Tsigaridis and Kanakidou, 2007; Kanakidou et al., 2016, 2020; Myriokefalitakis et al., 2015, 2016). Uncertainties in the simulations resulting from the use of different emission databases have been investigated by Daskalakis et al. (2015). The model considers lognormal aerosol distributions in fine and coarse modes and allows hygroscopic growth of particles, as well as removal by large-scale and convective precipitation and gravitational settling. In-cloud and below-cloud scavenging are parameterized in TM4-ECPL as described in detail by Jeuken et al. (2001). In-cloud scavenging of water-soluble gases accounts for the solubility of the gases (effective Henry law coefficients; Myriokefalitakis et al., 2011; Tsigaridis et al., 2006 and references therein). Details on the emissions used in the model are provided in Myriokefalitakis et al. (2015, 2016) and Kanakidou et al. (2020). Dust emissions are calculated online as described by Tegen et al. (2002) and implemented as in Van Noije et al. (2014). Dust aerosol (including feldspar and quartz) emissions are represented by lognormal distributions in fine and coarse modes with dry mass median radii (lognormal standard deviation) of 0.34µm (1.59) and 1.75µm (2.00), respectively and particle density is equal to 2650 kg.m⁻³ (Ginoux et al., 2004; Tegen et al., 2002). We assume that all aerosols are externally mixed. Typical lognormal distribution equations are used to convert mass to number concentration of aerosols in each grid box of the model.

2.2 K-feldspar and quartz emissions

To calculate the quartz and K-feldspar emissions we use the global soil mineralogy atlas of Claquin et al. (1999), including the updates proposed in Nickovic et al. (2012). The atlas of Claquin et al. (1999) provides mineral fractions for eight major minerals, including quartz and feldspar, in arid and semi-arid regions for two soil size fractions: clay (up to 2µm) and silt (from 2 to 50µm). Claquin et al. (1999) exclusively apportion feldspar to the silt size fraction, but feldspar is also observed in the smaller sizes, both in the soil (e.g. Journet et al., 2014) and the airborne dust (e.g. Kandler et al., 2009). Following Atkinson et al. (2013) we added feldspar in the clay size fraction of the soil by scaling the feldspar fraction in the silt size fraction of the

4

240 soil with the clay-to-silt ratio of quartz. Since Claquin et al. (1999) only estimated total feldspar, based on observations, we also assumed that K-feldspar represents 35% of feldspar (Atkinson et al., 2013).

Atkinson et al. (2013) calculated the emission of K-feldspar as the product of dust emission flux and the soil fractions of K-feldspar. Here, we additionally account for the known differences between soil and emitted mineral fractions. The soil samples that constitute the basis of soil mineralogical atlases are subject to destructive analytical techniques. As a result, the aggregates 245 originally present in the soil are more effectively disturbed than through wind erosion processes, hence overemphasizing the fine fraction of clay minerals compared to their actual abundance at emission (Perlwitz et al., 2015a). We calculated the emitted mass fractions of quartz and K-feldspar in the fine and coarse modes based on Brittle Fragmentation Theory (BFT) from Kok (2011). BFT restores soil clay-sized minerals (mainly illite, kaolinite and smectite), created by wet sieving, into emitted coarse aggregates. As a consequence, the fractional contribution of quartz and K-feldspar in the emitted coarse dust is reduced relative 250 to their fractions in the silt size of the soil (Pérez García-Pando et al., 2016; Perlwitz et al., 2015a, b). Finally, the corresponding accumulation and coarse-mode emission of each mineral is calculated by applying the respective mineral emitted mass fractions to the dust emission flux.

2.3 Calculation of INP concentrations

The influence of mineralogy on INP concentrations is parameterized in TM4-ECPL using the singular approximation of ice-255 nucleating activities of aerosols and based on laboratory-derived active site parameterizations provided in Harrison et al. (2019). These are good approximations for the majority of feldspars and quartz studied in the laboratory. The parameterization for K-feldspar is valid between -3.5°C and -37.5°C and captures the observed plateau in active sites density ($n_s(T)$) below −30°C, reproducing higher $n_s(T)$ values at temperatures warmer than −10 °C. In addition, Harrison et al. (2019) provide a new parameterization for quartz minerals to constrain their role as INP that is valid for a temperature range from −10.5 to -37.5°C. 260 In this study, the parameterizations are exclusively applied within the valid temperature limits since outside these limits, the parameterizations yield non-realistic results. These parameterizations have an uncertainty, expressed as the standard deviation for $\log(n_s(T))$, of about 0.8 for both quartz and K-feldspar INPs that corresponds to an order of magnitude in their concentrations. Part of this uncertainty is derived from impurities that influence how individual quartz samples fracture, impacting the presence of active sites (Harrison et al., 2019). As discussed in the introduction, the ice-nucleating ability of the 265 different minerals is determined from laboratory experiments using artificial mineral samples (Kumar et al., 2018), which may not be representative of realistic atmospheric conditions. Also, data analysis provided in Atkinson et al. (2013) suggests that aggregation of feldspar particles resulting in reduced surface area is at most a minor effect in the ice nucleuation efficiency compared with the differences in active sites density of different types of K-feldspar (factor of 6) (Harrison et al., 2016). Additionally, considerable differences in simulated INP numbers using laboratory-based and field-based INP 270 parameterizations are attributed to biological nanoscale fragments attached to mineral dust particles (O'Sullivan et al., 2016). These effects are not considered in the present study.

The ice nucleation active surface site density that is derived by the spectrum of ice-nucleating properties and for a polydisperse aerosol sample is given by the Poisson distribution: (1)

$$IN(T) = \sum_i \sum_j n_{i,j} \{1 - exp[-S_{i,j}\, n_s(T)]\}$$

275 Where IN is the ice number concentration formed on the aerosol based on parameterizations provided in Harrison et al. (2019), $n_{i,j}$ is the total aerosol number concentration, where indexes i, j correspond to aerosol type (quartz or K-feldspar) and size mode (accumulation or coarse mode), respectively. $S_{i,j}$ is the individual aerosol particle mean surface area in size mode j and (see Niemand et al. (2012) for details).

In order to estimate aerosol surface area, we assume that each mineral dust particle is spherical and externally mixed (Atkinson 280 et al., 2013; Vergara-Temprado et al., 2017). As discussed in Harrison et al. (2019), Atkinson et al. (2013) found that fully

5

internally mixed feldspar particles produce the same INP concentrations with externally mixed particles at temperatures above

315 -25°C but lead to higher INP concentrations by one to two orders of magnitude at the lowest temperatures of validity of the parameterization. In addition, in the present study, removal mechanisms by physical processes are applied directly to all dust particles such as sedimentation, deposition and scavenging and not preferentially to INPs.

There are two different ways to represent simulated INP concentrations by the model, either as potential INP that can activate to ice at a fixed temperature ($[INP]_T$) or as ambient INP that are calculated to be active in the model's ambient local atmospheric

320 temperature. $[INP]_{ambient}$ is a useful way of looking at the INP concentration relevant to non-deep convective mixed-phase clouds, while $[INP]_T$ can be an indicator for the distribution of INPs concentrations at temperatures that will affect clouds with vertical extent like deep-convective systems (Vergara-Temprado et al., 2017) as illustrated in Figure 1. Additionally, because most measurements are made by exposing particles to specific temperatures depending on instrumentation, $[INP]_T$ is a pertinent quantity when comparing modelled and observed INP concentrations.

325

3. Evaluation of dust and INP simulations

3.1 Dust

Airborne dust concentration is of paramount importance to this work, since dust affects directly the amount of INP in the atmosphere. Consequently, we evaluate modelled dust by comparing with monthly averaged dust observations from stations

330 that are in the outflow of Saharan desert and with worldwide climatological observations. The climatological annual means comparison allows us to validate the geographical distribution of sources and transported dust regions, while the monthly means comparison reveals if the intra-annual variability can be well captured by the model.

We first evaluate the dust mass simulations against monthly averaged dust observations at nine ground-based stations between 2000 and 2017. Supplementary Figure S1 shows the location of these stations plotted over the simulated dust concentration

335 for summer 2015. All stations are in areas suitable for studying emissions of Saharan dust and its atmospheric transport. Four stations (M'Bour, Bambey, Cinzana, and Banizoumbou) are located at the edge of the Sahel, the major natural dust source of the region (Lebel et al., 2010), three stations (Miami, Barbados and Cayenne) are on the American continent downwind the dust Atlantic transport (Zuidema et al., 2019; Prospero et al., 2020) and two stations, Finokalia (Crete, Greece) (Mihalopoulos et al., 1997; Kalivitis et al., 2007), and Agia Marina (Cyprus) (Kleanthous et al., 2014; Pikridas et al., 2018) lie on the dust

340 transport route crossing the Mediterranean. Figure 2 depicts the comparison of model dust aerosol concentrations with observations on a monthly mean basis (correlation coefficient, R=0.81). The methodology to derive dust concentrations from the aerosol observations at these sites is discussed in the supplement. The mean bias between model and observations is 8.3 $\mu g \cdot m^{-3}$. The total average dust concentration observed at the selected locations and during the studied period 2000-2017 is approximately 43.3 $\mu g \cdot m^{-3}$. Thus, the mean bias corresponds to 5% of the total concentration. The relative error increases with

345 decreasing concentrations, and only a few outliers are not within one order of magnitude of the observations in Figure 2, mainly corresponding to observations at the Caribbean and American stations.

We further evaluate modelled dust by comparing with climatological globally distributed observations of dust surface concentration and deposition for the years from 2009 to 2016 when we also perform the comparison between observed and modelled INP concentrations (see below, section 3.2). Climatological annual means of dust surface from the Rosenstiel School

350 of Marine and Atmospheric Science (RSMAS) of the University of Miami (Arimoto et al., 1995; Prospero, 1996, 1999) and the African Aerosol Multidisciplinary Analysis (AMMA) (Marticorena et al., 2010) are compared with the multi-annual model mean surface dust concentration (Figure 3a). We also compare the modelled deposition dust fluxes with the observations for modern climate compiled by Albani et al. (2014). Measurements from 110 different locations and the constrained mass fraction

6

Deleted: partially internally

Deleted: modelled

Deleted: (Figure S4).

Deleted: and Agia Marina (Cyprus) (Pikridas et al., 2018; Kleanthous et al., 2014), lie on the dust transport route crossing the Mediterranean.

Deleted: Albani et al. (2014)

for particles with a diameter lower than 10μm to conform to the range of simulated sizes are compared to modeled deposition dust fluxes (Figure 3b). Table S1 summarizes the statistical parameters used to validate the model, and the locations (and regions) of the various observations are depicted in Figure S2. The correlation coefficient (R) reveals the linear relationship between model results and observations, while the normalized mean bias (nMB), and the normalized root-mean-square error (nRMSE) are the measure of the mean deviation of the model from the observations due to random and systematic errors. All the equations that are used for the statistical analysis of model results are provided in the Supplement (Eqs. S1–S3).

The geographical distribution of the available concentration stations (23 in total) in Figure 3a covers locations close to emission sources (AMMA stations over the Sahelian dust transect), and in both transport and remote regions (RSMAS). The overestimation of the dust surface concentration already shown at the monthly scale is also observed in the comparison with annual mean climatological observations, with an overall normalized mean bias of 44.1%. Errors are generally larger after transport to remote regions, particularly over the North Pacific, than over source regions (Figure 3a). When it comes to deposition, the errors are larger than in the representation of the surface concentration fields, particularly overestimations are found over the Southern Ocean and Arctic, than downwind sources (Figure 3b); while concentrations over Europe and South America are largely underestimated. They are, however, kept within the one-order of magnitude differences, except for those points located over the Southern Ocean, where overestimations are significant. The aerosol concentrations and deposition fluxes in such remote regions are usually low and thus, small differences are emphasized in relative terms. There may be multiple causes for the discrepancy between modelled and observed fluxes (e.g. an excessive modelled fine fraction of aerosols, differences in the wet deposition fluxes caused by differences in precipitation, differences in the observed and modelled period, or uncertainties associated to the observations themselves). The main purpose of this comparison is to assess the ability of the model to reproduce the geographical distribution of dust in the atmosphere, which is found satisfactory, and exploring further the issues behind the deviation in a particular remote region is out of the scope of this work.

3.2 INP

In Figure 4, we compare the INP concentrations calculated by the TM4-ECPL model with available INP observations from the databases of BACCHUS (Impact of Biogenic versus Anthropogenic emissions on Clouds and Climate: towards a Holistic UnderStanding) (http://www.bacchus-env.eu/in/index.php, last access on March 2019) and Wex et al. (2019) (https://doi.pangaea.de/10.1594/PANGAEA.899701, last access on February 2022). These data span the years 2009 to 2016 and originate from different campaigns (locations are shown in supplementary Figure S3). For this comparison, $[INP]_T$ concentrations are calculated at the temperature at which measurements were performed. All model results are compared to observations for the specific month and year of the observations, except the observed dataset by Yin et al.(2012), which covers temporally scattered measurements (between 1963 to 2003). This dataset is compared to the modeled multi-annual monthly mean INP concentration considering the years 2009 to 2016. The color bar shows the corresponding temperature at which the measurement is performed (Figure 4a) or the modeled dust aerosol mass concentration (Figure 4b). These different color bars allow us to determine if the bias of the model can be correlated with the temperature of the observed INP (e.g., highly active INP reddish symbols in Figure 4a) or with modelled dust mass (e.g., low modelled dust mass, blueish symbols in Figure 4b). The model agrees reasonably well with observations of INP (R=0.84, Table S2) at the full temperature range of the measurements when dust is present in significant amounts (dust concentrations larger than 10^{-1} µg m^{-3}) (Figure 4b) and at temperatures lower than -10°C (Figure 4a). Overall, the model reproduces about 51% of the observations within an order of magnitude and about 69% within one and a half orders of magnitude (Table S2).

7

The model is not efficient enough in simulating highly ice-active INP observed in both Wex (triangles) and BACCHUS (circles) databases (Figure 4a, red spots corresponding to high temperatures). The temperature range of these measurements is very close to the temperature limits of the Harrison et al. (2019) parameterization. Since the quartz parameterization temperature limit is at -10.5°C, INP observations measured between -3.5 and -10.5°C are compared with simulated INP derived from K-feldspar only. Supplementary Figure S4 depicts the comparison to observations using quartz and K-feldspar separately. This figure reveals that INP from quartz can improve the comparison with observations at low temperatures, which is consistent with the suggestion of Boose et al. (2016) that for temperatures between -33°C to -37°C, quartz can be a significant contributor to INP concentration. Figure S4d clearly shows that consideration of quartz together with K-feldspar INP improves the comparison with observations by moving the respective points closer to the 1:1 line. This is particularly true for high INP concentrations at low temperatures (below -30°C) and for relatively low INP concentrations at temperatures around -20°C. Overall about 3% more data points are within 1.5 orders of magnitude from the observations when accounting for quartz INP in addition to feldspar INP (Table S2). Additionally, modeled INP concentrations are strongly underestimated compared to observations for temperatures above -25°C. Si et al. (2019) pointed out that mineral dust was a major contributor to the INP population at temperatures lower than -25°C. They also found that, for three coastal sites, modeled INP concentrations based on K-feldspar as the only INP precursor agreed well with INP measurements at -25°C, but measurements at −15°C were underestimated, indicating a missing source of INP that activates at temperatures higher than -25°C. These results on the importance of dust as INP for different temperature ranges agree with our study as can also be seen in Supplementary Figure S4c.

Figure 4b reveals that the observed high concentrations of INP correspond to high dust mass concentrations. Additionally, the observed low concentrations of INP correspond to particles that activate at relatively high temperatures (higher than -10°C; reddish symbols in Figure 4a) and low mass dust concentration (blueish symbols in Figure 4b). Thus, our model underestimates measurements corresponding to low dust mass concentrations (blueish symbols in Figure 4b). As shown in Figure 4a, these low-dust mass points correspond to measurements performed at temperatures around -20°C and -25°C. Therefore, these INP observations not reproduced by our model when accounting only for dust-originating INP are probably not solely affected by airborne mineral dust, pointing to other aerosol sources contributing to INP as discussed below.

Supplementary Figure S5 depicts globally the regions and months where the model overestimates (blueish) and underestimates (reddish) INP observations. Improving the representation of the dust cycle could reduce the bias of INP simulations. The model underestimate of the dust surface concentrations observations over Europe and Southern Ocean and the dust deposition fluxes over South Africa and Western Asia, discussed in section 3.1, may at least partly explain the underestimation by the model of the observed INP concentrations (close to 2 orders of magnitude, reddish points) in these regions, as depicted in Supplementary Figure S5. Additionally, model deviation from measurements could be attributed to potential inaccuracies in the simulated content of quartz and K-feldspar due to uncertainties in the dust cycle and in the emitted mineral fractions (Perlwitz et al., 2015a; Pérez García-Pando et al., 2016). Furthermore, the boxes in Supplementary Figure S5 depict the climatological monthly mean bias (observations – model) at specific regions (Arctic, Europe, China, North America, Central America, North Africa, South Africa and West Asia-Middle East). This analysis shows that observed INP concentrations are underestimated by 2 orders of magnitude over Europe during autumn and over West Asia-Middle East during autumn and winter.

The overall agreement between the model results and observations is reasonable (see also Supplementary Table S2), but there are significant discrepancies. These differences between model results and observations could be attributed to several factors, such as the omission of the contribution of marine organic (Wilson et al., 2015) and terrestrial biogenic aerosols (Myriokefalitakis et al., 2021; Spracklen and Heald, 2014). Ice nucleation at temperatures in the vicinity of zero is typically

related to macromolecules from biogenic entities such as bacteria, fungal spores, pollen, and marine biota. These ice-active macromolecules nucleate ice from just below 0°C down to roughly −20°C (O'Sullivan et al., 2018; Kanji et al., 2017; Murray et al., 2012). Indeed, based on air mass back-trajectories analysis, Wex et al. (2019) (triangles in Fig 4a) suggested that both terrestrial locations in the Arctic and the adjacent sea were possible source areas for highly active INPs derived from material of biogenic origin. In addition, mineral dust particles likely only become ice active at low temperatures (see section 2.3), but they may be carriers of biogenic ice-active macromolecules (O'Sullivan et al., 2014; Hill et al., 2016; O'Sullivan et al., 2016), which enhance dust nucleation activity at higher temperatures. Thus, although some biological nanoscale fragments could be attached to mineral dust particles (Froehlich-Nowoisky et al., 2015; Violaki et al., 2021; O'Sullivan et al., 2016), their effect on the ice nucleating activity of dust was not considered here. Furthermore, errors may be partly due to atmospheric processes such as ageing, resulting in ice ability degradation (leading to positive model bias) or a possible underestimation of the concentration of these transported aerosol species (leading to negative model bias). These processes are currently neglected in our model but the sensitivity of the INP simulations to these uncertainties is the subject of an ongoing complementary study.

4. K-feldspar and quartz contributions to the global INP distribution

Figure 5a presents the simulated distributions of K-feldspar and quartz particles present at an atmospheric pressure level of 600 hPa that are able to freeze in the immersion mode at -20°C and form ice crystals, hereafter called [INP]$_{-20}$. These conditions are representative of mixed-phase clouds' glaciation and allow both quartz and K-feldspar to activate and act as INP. [INP]$_{-20}$ distributions are of interest for their impact on clouds formed in deep-convective systems experiencing large vertical velocities (Figure 1). They are mainly observed in subtropical and tropical regions. [INP]$_{-20}$ concentrations derived from K-feldspar and quartz (Figure 5a) contribute much more to mid-latitude, mid-level mixed-phase clouds in the Northern Hemisphere (NH) than in the Southern Hemisphere (SH) due to the location of dust sources and long-range atmospheric transport patterns that favor dust concentration in the NH. However, there are also dust-related INP sources in the SH, such as those from Patagonia, South Africa and west Australia, that yield considerable [INP]$_{-20}$ concentrations (larger than 10^{-2} L^{-1}).

To investigate the spatial variability of the contribution of each mineral to potential primary ice crystals concentration at -20°C, we also present the ratio of INP from quartz ([INP]$_{quartz}$) to the INP derived from both quartz and K-feldspar ([INP]$_{total}$) at that temperature (Figure 5b). This analysis shows regions at the pressure level of 600hPa and temperature of -20°C where [INP]$_{quartz}$ has the potential to significantly contribute to the total ice crystals concentration derived by immersion freezing on dust particles, in particular we attribute to quartz 30% of the total [INP]$_{total}$ over North Atlantic, south USA and more than 40% over India and Eurasia.

The areas most affected by ice crystals derived from quartz are the regions of the South Saudi Arabian Peninsula, India, North Indonesia and Eurasia (Figure 5b), where high ratios of quartz minerals to dust mass (Figure 5d) and high concentrations of derived ice crystals of about 0.5 L^{-1} are simulated (Figure 5a). The mass contribution of quartz to the dust particles originating from Saudi Arabia and the Gobi Deserts exceeds 35% (Figure 5d). At the same time, the quartz contribution to ice crystals formed by immersion freezing on dust particles is 35-40% (Figure 5b). When the mass of quartz is six times that of feldspar (Figure 6), the quartz derived ice crystal concentration ([INP]$_{quartz}$) constitutes more than 35-45% of total ice crystals concentration derived from dust (Figure 5b). Furthermore, the North Atlantic and, generally, the NH are likely affected by ice formation from both quartz and K-feldspar. In contrast, the South Atlantic is affected by K-feldspar INP originating from the Patagonia desert since 75% of ice crystals potentially formed at -20°C are derived from K-feldspar, and the remaining 25% is from quartz (Figure 5b). Additionally, high percentages of quartz minerals and low feldspar (about 6%) in terms of mass are calculated over South Africa originating from the Kalahari Desert. There 35% of the total INP concentrations (around 10^{-2} L^{-1}) originate from quartz particles (Figures 5c-d).

As expected, concentrations of primary ice crystals derived from dust at the model temperature, [INP]$_{ambient}$, follow the air temperature distribution, showing the highest modeled values roughly poleward of 50 degrees in both hemispheres (Figure 7 for model dust concentrations and temperature at 600 hPa). The contributions of both minerals to primary ice crystals are

635 comparable (Figure 7c-d); [INP]$_{quartz}$ appears as important as [INP]$_{feldspar}$ around 40° and poleward of 70°. Overall, the number concentration of primary ice formed by immersion freezing on dust particles strongly depends on the ambient temperature and the mass concentrations of these minerals, with positive dependence on mass and negative dependence on temperature.

Figure 8a shows the annual zonal mean distribution of primary ice crystals derived from both minerals. Total primary ice
640 crystals ([INP]$_{total}$) maximize approximately at 600-500 hPa below -25 °C in mid-latitudes at local model temperature (Figure 8a), with K-feldspar-derived ice crystals accounting for the largest fraction (Figure 8b). This behavior is attributed to the high ice activity of K-feldspar and its temperature dependence. However, at lower altitudes and below -12°C, low [INP]$_{total}$ concentrations (<10^{-2} L^{-1}) are calculated and are mainly derived from quartz dust particles (60%) (Figure 8b). This outcome is attributed to quartz's high number concentration between 30-40°N at and below 700 hPa, partially associated with higher local
645 quartz than feldspar emissions from Asian dust sources (Claquin et al.,1999; Nickovic et al., 2012). At temperatures below −25 °C, the quartz contribution becomes increasingly important with increases in INP concentration when the temperature decreases, reaching up to 50 % at −35 °C (Figure 8b). These findings agree well with Ilić et al. (2022) and Boose et al. (2016), who showed that quartz could significantly contribute to [INP] at temperatures between the homogeneous freezing limit and −33°C. Overall, [INP]$_{quartz}$ dominates at the lowest and the highest altitudes of dust-derived INP (Figure 8b; reddish colors).
650 This is clearly demonstrated in Supplementary Figure S6 for Eurasia where at the range of 700-900hPa and around 450 hPa model pressure levels the contribution of [INP]$_{quartz}$ to total ice crystals from immersion freezing on dust particles exceeds 60%. Figure S7 shows that in the South Hemisphere quartz contribution to total INP is about 40%. Consequently, [INP]$_{feldspar}$ is expected to affect mid-altitude clouds, while [INP]$_{quartz}$ is expected to affect both the low-altitude clouds and the high-altitude cold clouds. The present study emphasizes that INP concentrations could be significantly affected not only by K-feldspar, as
655 generally thought but also by quartz. The evaluation of the climate impact of these INPs is a subject of ongoing research. It requires the incorporation of parameterizations, such as those used here, into a climate model able to simulate ice formation and its interactions within the climate system.

5. Conclusions

The contribution of K-feldspar and quartz dust minerals as ice-nucleating particles has been investigated in this study using a
660 three-dimensional global chemistry transport model as a first step towards their incorporation in a climate model. Laboratory-derived parameterizations based on the singular description and aerosol chemical composition have been incorporated into the model together with an explicit representation of the dust mineralogy that considers regional variations in the composition of the dust sources and relies on the Brittle Fragmentation Theory to derive the size-distributed mineral abundances in the atmosphere. To our knowledge, this is the first time a global chemistry transport model considers the contribution of both
665 quartz and K-feldspar to predict INP concentrations.

Quartz particles have lower ice active density (Harrison et al., 2019) but are more abundant in airborne dust than K-feldspar, thus partly compensating for their lower ice nucleating activity with respect to K-feldspar. We find that [INP]$_{quartz}$ dominates at lower altitudes over locations with abundant dust emissions but low INP concentrations. There are regions of the
670 atmosphere, in particular over mid-and high-latitudes of Asia, where quartz contributes over 60% (at ambient model temperature) to the total INP concentration derived from dust aerosols represented by quartz and K-feldspar. The quartz

10

contribution increases when temperature is decreasing, resulting in high INP concentrations at temperatures below about −30°C and high altitudes. Consideration of quartz-derived INP improves the comparison with observations for high INP concentrations at low temperatures (below about -30ºC) and relatively low INP concentrations at temperatures around -20ºC. These results highlight the important role of quartz in increasing INP concentrations, mainly over the mid-to-high latitudes of both hemispheres.

Overall, the simulated concentrations of INP from two-dust components agree with the observational data from the BACCHUS and Wex et al. (2019) databases within one and a half orders of magnitude. Statistical analysis of the comparison of the modeled annual mean dust surface concentration has shown that the model underestimates dust concentration over Europe and the Southern Ocean, potentially explaining part of the bias between modeled and observed INP concentrations. Furthermore, the omission of marine and terrestrial biological INP sources, dust mineralogy uncertainties and atmospheric processes such as ageing and in-cloud removal could also explain the model's discrepancies. The evaluation of the importance of these factors on INP simulated number concentrations is the topic of ongoing studies. As importantly, the heterogeneously formed ice crystals could trigger secondary ice production processes, such as the Hallett – Mossop process, which usually takes place around -5ºC and could probably improve our comparison at high temperatures. These processes are not considered in our study. However, they are known to further increase the number concentration of ice crystals (Sotiropoulou et al., 2020) and their subsequent climate impact.

We conclude that dust particles appear to be important precursors of INP, able to account for most of the observed INP number concentration globally. K-feldspar contributes globally most of the INP associated with desert dust because it is more ice-active and less sensitive than quartz to ageing processes that reduce the ice-nucleating activity of the particles (Harrison et al., 2019). However, we highlight that INP concentrations could also be significantly affected by quartz particles, which are abundant in airborne dust. Improving the representation of INP thus requires further constraining the abundance of quartz and K-feldspar in arid soil-surfaces along with their abundance, size distribution and mixing state in the emitted dust atmospheric particles at global scale. Also, additional experimental studies on the ice-nucleating ability of mineral dust particles must be performed to investigate the impact of atmospheric ageing and the presence of biological fragments attached to dust on the ice-nucleating activity of dust particles.

11

Midi-Pyrénées and the Observatoire des Sciences de l'Univers EFLUVE, and M. Pikridas from Climate and Atmosphere Research Center of The Cyprus Institute

Data availability

The INP data used in this study can be accessed through BACCHUS (http://www.bacchus-env.eu/in/info.php? id=71) and (frozen fractions and INP concentrations) on Pangaea (https://doi.pangaea.de/10.1594/ PANGAEA.899701; Wex et al., 2019). Model output will be available on zenodo before publication of the paper.

Authors' contributions

MK and MC conceived the study; MC modified the model to account for INP and performed the simulations, visualized and analyzed data, and wrote the initial version of the manuscript; MK supervised the work with feedback from AN and CPG-P and re-edited the manuscript; SM implemented the dust emissions module and the initial dataset of dust mineralogy in the model; ND, MZ, MV and MGA evaluated the dust simulations; NK provided characterized dust aerosol observations from Finokalia station; MC-S provided key feedback on the implementation of the ice nucleation active surface site density parameterization; CPG-P and MGA provided the emitted mineral fractions of quartz and feldspar; CPG-P re-edited parts of the manuscript; all authors read and commented the manuscript.

References

Abdelkader, M., Metzger, S., Steil, B., Klingmüller, K., Tost, H., Pozzer, A., Stenchikov, G., Barrie, L., and Lelieveld, J.: Sensitivity of transatlantic dust transport to chemical aging and related atmospheric processes, Atmos. Chem. Phys., 17, 3799–3821, https://doi.org/10.5194/acp-17-3799-2017, 2017.

Albani, S., Mahowald, N. M., Perry, A. T., Scanza, R. A., Zender, C. S., G.Heavens, N., V. Maggi, J. F. K., and L.Otto-Bliesner, and B.: Improved dust representation in the CommunityAtmosphere Model, J. Adv. Model. Earth Syst., 6, 92–95, https://doi.org/10.1002/2013MS000279.Received, 2014.

Atkinson, J. D., Murray, B. J., Woodhouse, M. T., Whale, T. F., Baustian, K. J., Carslaw, K. S., Dobbie, S., O'Sullivan, D., and Malkin, T. L.: The importance of feldspar for ice nucleation by mineral dust in mixed-phase clouds, Nature, 498, 355–358, https://doi.org/10.1038/nature12278, 2013.

Barahona, D. and Nenes, A.: Parameterizing the competition between homogeneous and heterogeneous freezing in ice cloud formation - Polydisperse ice nuclei, Atmos. Chem. Phys., 9, 5933–5948, https://doi.org/10.5194/acp-9-5933-2009, 2009.

Boucher, O.: Atmospheric Aerosols. Properties and Climate Impacts, Springer Netherlands, Dordrecht, Heidelberg, New York, London, 311 pp., https://doi.org/10.1007/978-94-017-9649-1, 2015.

Burrows, S. M., McCluskey, C. S., Cornwell, G., Steinke, I., Zhang, K., Zhao, B., Zawadowicz, M., Raman, A., Kulkarni, G., China, S., Zelenyuk, A., and DeMott, P. J.: Ice-Nucleating Particles That Impact Clouds and Climate: Observational and Modeling Research Needs, https://doi.org/10.1029/2021RG000745, 16 June 2022.

Daskalakis, N., Myriokefalitakis, S., and Kanakidou, M.: Sensitivity of tropospheric loads and lifetimes of short lived pollutants to fire emissions, Atmos. Chem. Phys., 15, 3543–3563, https://doi.org/10.5194/acp-15-3543-2015, 2015.

Daskalakis, N., Tsigaridis, K., Myriokefalitakis, S., Fanourgakis, G. S., and Kanakidou, M.: Large gain in air quality compared to an alternative anthropogenic emissions scenario, Atmos. Chem. Phys., 16, 9771–9784, https://doi.org/10.5194/acp-16-9771-2016, 2016.

Daskalakis, N., Gallardo, L., Kanakidou, M., Nüß, J. R., Menares, C., Rondanelli, R., Thompson, A. M., and Vrekoussis, M.:

Impact of biomass burning and stratospheric intrusions in the remote South Pacific Ocean troposphere, Atmos. Chem. Phys.,
825   22, 4075–4099, https://doi.org/10.5194/acp-22-4075-2022, 2022.

Dee, D. P., Uppala, S. M., Simmons, A. J., Berrisford, P., Poli, P., Kobayashi, S., Andrae, U., Balmaseda, M. A., Balsamo, G., Bauer, P., Bechtold, P., Beljaars, A. C. M., van de Berg, L., Bidlot, J., Bormann, N., Delsol, C., Dragani, R., Fuentes, M., Geer, A. J., Haimberger, L., Healy, S. B., Hersbach, H., Hólm, E. V., Isaksen, L., Kållberg, P., Köhler, M., Matricardi, M., Mcnally, A. P., Monge-Sanz, B. M., Morcrette, J. J., Park, B. K., Peubey, C., de Rosnay, P., Tavolato, C., Thépaut, J. N., and
830   Vitart, F.: The ERA-Interim reanalysis: Configuration and performance of the data assimilation system, Q. J. R. Meteorol. Soc., 137, 553–597, https://doi.org/10.1002/qj.828, 2011.

DeMott, P. J., Prenni, A. J., Liu, X., Kreidenweis, S. M., Petters, M. D., Twohy, C. H., Richardson, M. S., Eidhammer, T., and Rogers, D. C.: Predicting global atmospheric ice nuclei distributions and their impacts on climate, Proc. Natl. Acad. Sci. U. S. A., 107, 11217–11222, https://doi.org/10.1073/pnas.0910818107, 2010.

835   Fan, J., Wang, Y., Rosenfeld, D., and Liu, X.: Review of aerosol-cloud interactions: Mechanisms, significance, and challenges, J. Atmos. Sci., 73, 4221–4252, https://doi.org/10.1175/JAS-D-16-0037.1, 2016.

Fan, J., Ruby Leung, L., Rosenfeld, D., and Demott, P. J.: Effects of cloud condensation nuclei and ice nucleating particles on precipitation processes and supercooled liquid in mixed-phase orographic clouds, Atmos. Chem. Phys., 17, 1017–1035, https://doi.org/10.5194/acp-17-1017-2017, 2017.

840   Field, P. R., Lawson, R. P., Brown, P. R. A., Lloyd, G., Westbrook, C., Moisseev, D., Miltenberger, A., Nenes, A., Blyth, A., Choularton, T., Connolly, P., Buehl, J., Crosier, J., Cui, Z., Dearden, C., DeMott, P., Flossmann, A., Heymsfield, A., Huang, Y., Kalesse, H., Kanji, Z. A., Korolev, A., Kirchgaessner, A., Lasher-Trapp, S., Leisner, T., McFarquhar, G., Phillips, V., Stith, J., and Sullivan, S.: Chapter 7. Secondary Ice Production - current state of the science and recommendations for the future, Meteorol. Monogr., 1–20, https://doi.org/10.1175/amsmonographs-d-16-0014.1, 2016.

845   Froehlich-Nowoisky, J., Hill, T. C. J., Pummer, B. G., Yordanova, P., Franc, G. D., and Poeschl, U.: Ice nucleation activity in the widespread soil fungus Mortierella alpina, 12, 1057–1071, https://doi.org/10.5194/bg-12-1057-2015, 2015.

Georgakaki, P., Sotiropoulou, G., Vignon, É., Billault-Roux, A.-C., Berne, A., and Nenes, A.: Secondary ice production processes in wintertime alpine mixed-phase clouds, Atmos. Chem. Phys., 22, 1965–1988, https://doi.org/10.5194/acp-22-1965-2022, 2022.

850   Ghan, S. J., Abdul-Razzak, H., Nenes, A., Ming, Y., Liu, X., Ovchinnikov, M., Shipway, B., Meskhidze, N., Xu, J., and Shi, X.: Droplet nucleation: Physically-based parameterizations and comparative evaluation, J. Adv. Model. Earth Syst., 3, 1–34, https://doi.org/10.1029/2011ms000074, 2011.

Ginoux, P.: Atmospheric chemistry: Warming or cooling dust?, Nat. Geosci., 10, 246–247, https://doi.org/10.1038/ngeo2923, 2017.

855   Ginoux, P., Prospero, J. M., Torres, O., and Chin, M.: Long-term simulation of global dust distribution with the GOCART model: Correlation with North Atlantic Oscillation, Environ. Model. Softw., 19, 113–128, https://doi.org/10.1016/S1364-8152(03)00114-2, 2004.

Harrison, A. D., Whale, T. F., Carpenter, M. A., Holden, M. A., Neve, L., O'Sullivan, D., Vergara Temprado, J., and Murray, B. J.: Not all feldspars are equal: A survey of ice nucleating properties across the feldspar group of minerals, Atmos. Chem.
860   Phys., 16, 10927–10940, https://doi.org/10.5194/acp-16-10927-2016, 2016.

Harrison, A. D., Lever, K., Sanchez-Marroquin, A., Holden, M. A., Whale, T. F., Tarn, M. D., McQuaid, J. B., and Murray, B. J.: The ice-nucleating ability of quartz immersed in water and its atmospheric importance compared to K-feldspar, Atmos. Chem. Phys. Discuss., 1–23, https://doi.org/10.5194/acp-2019-288, 2019.

Hill, T. C. J., Demott, P. J., Tobo, Y., Fröhlich-Nowoisky, J., Moffett, B. F., Franc, G. D., and Kreidenweis, S. M.: Sources of
865   organic ice nucleating particles in soils, Atmos. Chem. Phys., 16, 7195–7211, https://doi.org/10.5194/acp-16-7195-2016, 2016.

Holden, M. A., Whale, T. F., Tarn, M. D., O'Sullivan, D., Walshaw, R. D., Murray, B. J., Meldrum, F. C., and Christenson,

H. K.: High-speed imaging of ice nucleation in water proves the existence of active sites, Sci. Adv., 5, 1–11, https://doi.org/10.1126/sciadv.aav4316, 2019.

870 Hoose, C. and Möhler, O.: Heterogeneous ice nucleation on atmospheric aerosols: A review of results from laboratory experiments, 9817–9854 pp., https://doi.org/10.5194/acp-12-9817-2012, 2012.

Hoose, C., Kristjánsson, J. E., and Burrows, S. M.: How important is biological ice nucleation in clouds on a global scale?, Environ. Res. Lett., 5, 024009, https://doi.org/10.1088/1748-9326/5/2/024009, 2010.

Ilić, L., Jovanović, A., Kuzmanoski, M., Lazić, L., Madonna, F., Rosoldi, M., Mytilinaios, M., Marinou, E., and Ničković, S.: Mineralogy Sensitive Immersion Freezing Parameterization in DREAM, J. Geophys. Res. Atmos., 127, 1–22, 875 https://doi.org/10.1029/2021JD035093, 2022.

IPCC: IPCC, 2021: Climate Change 2021. The Physical Science Basis. Summary for Policymakers., edited by: Masson-Delmotte, V., P. Zhai, A. Pirani, S. L. Connors, C. Péan, S. Berger, N. Caud, Y. Chen, L. Goldfarb, M. I. Gomis, M. Huang, K. Leitzell, E. Lonnoy, J. B. R. Matthews, T. K. Maycock, T. Waterfield, O. Yelekçi, R. Yu and B. Zhou , Masson-Delmotte, V., R. Y. and B. Z., Cambridge University Press, Cambridge, United Kingdom and New York, NY, USA, 2021.

880 Iwata, A. and Matsuki, A.: Characterization of individual ice residual particles by the single droplet freezing method: A case study in the Asian dust outflow region, Atmos. Chem. Phys., 18, 1785–1804, https://doi.org/10.5194/acp-18-1785-2018, 2018.

Jeuken, M., Van Wijk, R., Peleman, J., and Lindhout, P.: An integrated interspecific AFLP map of lettuce (Lactuca) based on two L. sativa × L. saligna F2 populations, Theor. Appl. Genet., 103, 638–647, https://doi.org/10.1007/s001220100657, 2001.

Kalivitis, N., Gerasopoulos, E., Vrekoussis, M., Kouvarakis, G., Kubilay, N., Hatzianastassiou, N., Vardavas, I., and 885 Mihalopoulos, N.: Dust transport over the eastern mediterranean derived from total ozone mapping spectrometer, aerosol robotic network, and surface measurements, J. Geophys. Res. Atmos., 112, https://doi.org/10.1029/2006JD007510, 2007.

Kanakidou, M., Myriokefalitakis, S., Daskalakis, N., Fanourgakis, G., Nenes, A., Baker, A. R., Tsigaridis, K., and Mihalopoulos, N.: Past, present, and future atmospheric nitrogen deposition, J. Atmos. Sci., 73, 2039–2047, https://doi.org/10.1175/JAS-D-15-0278.1, 2016.

890 Kanakidou, M., Myriokefalitakis, S., and Tsagkaraki, M.: Atmospheric inputs of nutrients to the Mediterranean Sea, Deep. Res. Part II Top. Stud. Oceanogr., 171, https://doi.org/10.1016/j.dsr2.2019.06.014, 2020.

Kandler, K., Schütz, L., Deutscher, C., Ebert, M., Hofmann, H., Jäckel, S., Jaenicke, R., Knippertz, P., Lieke, K., Massling, A., Petzold, A., Schladitz, A., Weinzierl, B., Wiedensohler, A., Zorn, S., and Weinbruch, S.: Size distribution, mass concentration, chemical and mineralogical composition and derived optical parameters of the boundary layer aerosol at Tinfou, 895 Morocco, during SAMUM 2006, Tellus B, 61, https://doi.org/10.3402/tellusb.v61i1.16798, 2009.

Kanji, Z. A., Ladino, L. A., Wex, H., Boose, Y., Burkert-Kohn, M., Cziczo, D. J., and Krämer, M.: Overview of Ice Nucleating Particles, Meteorol. Monogr., 58, 1.1-1.33, https://doi.org/10.1175/AMSMONOGRAPHS-D-16-0006.1, 2017.

Kanji, Z. A., Sullivan, R. C., Niemand, M., DeMott, P. J., Prenni, A. J., Chou, C., Saathoff, H., and Möhler, O.: Heterogeneous ice nucleation properties of natural desert dust particles coated with a surrogate of secondary organic aerosol, Atmos. Chem. 900 Phys., 19, 5091–5110, https://doi.org/10.5194/acp-19-5091-2019, 2019.

Kiselev, A., Bachmann, F., Pedevilla, P., Cox, S. J., Michaelides, A., Gerthsen, D., and Leisner, T.: Active sites in heterogeneous ice nucleation-the example of K-rich feldspars, Science (80-.)., 355, 367–371, https://doi.org/10.1126/science.aai8034, 2017.

Kleanthous, S., Vrekoussis, M., Mihalopoulos, N., Kalabokas, P., and Lelieveld, J.: On the temporal and spatial variation of 905 ozone in Cyprus, Sci. Total Environ., 476–477, 677–687, https://doi.org/10.1016/j.scitotenv.2013.12.101, 2014.

Kok, J. F., Ridley, D. A., Zhou, Q., Miller, R. L., Zhao, C., Heald, C. L., Ward, D. S., Albani, S., and Haustein, K.: Smaller desert dust cooling effect estimated from analysis of dust size and abundance, Nat. Geosci., 10, 274–278, https://doi.org/10.1038/ngeo2912, 2017.

Kumar, A., Marcolli, C., and Peter, T.: Ice nucleation activity of silicates and aluminosilicates in pure water and aqueous

14

Deleted: 2010a

Deleted: Hoose, C., Kristjánsson, J. E., and Burrows, S. M.: How important is biological ice nucleation in clouds on a global scale?, Environ. Res. Lett., 5, 24009, https://doi.org/10.1088/1748-9326/5/2/024009, 2010b.¶

Deleted: 2016

solutions. Part 2 &ndash; Quartz and amorphous silica, Atmos. Chem. Phys. Discuss., 1–35, https://doi.org/10.5194/acp-2018-1020, 2019.

Kumar, P., Sokolik, I. N., and Nenes, A.: Cloud condensation nuclei activity and droplet activation kinetics of wet processed regional dust samples and minerals, Atmos. Chem. Phys., 11, 8661–8676, https://doi.org/10.5194/acp-11-8661-2011, 2011.

920 Lance, S.: Coincidence errors in a cloud droplet probe (CDP) and a cloud and aerosol spectrometer (CAS), and the improved performance of a modified CDP, J. Atmos. Ocean. Technol., 29, 1532–1541, https://doi.org/10.1175/JTECH-D-11-00208.1, 2012.

Lebel, T., Parker, D. J., Flamant, C., Bourlès, B., Marticorena, B., Mougin, E., Peugeot, C., Diedhiou, A., Haywood, J. M., Ngamini, J. B., Polcher, J., Redelsperger, J. L., and Thorncroft, C. D.: The AMMA field campaigns: Multiscale and
925 multidisciplinary observations in the West African region, Q. J. R. Meteorol. Soc., 136, 8–33, https://doi.org/10.1002/qj.486, 2010.

Liu, X., Shi, X., Zhang, K., Jensen, E. J., Gettelman, A., Barahona, D., Nenes, A., and Lawson, P.: Sensitivity studies of dust ice nuclei effect on cirrus clouds with the Community Atmosphere Model CAM5, Atmos. Chem. Phys., 12, 12061–12079, https://doi.org/10.5194/acp-12-12061-2012, 2012.

930 Lohmann, U. and Diehl, K.: Sensitivity studies of the importance of dust ice nuclei for the indirect aerosol effect on stratiform mixed-phase clouds, J. Atmos. Sci., 63, 968–982, https://doi.org/10.1175/JAS3662.1, 2006.

Lohmann, U. and Gasparini, B.: A cirrus cloud climate dial?, Science (80-.)., 357, 248–249, https://doi.org/10.1126/science.aan3325, 2017.

Meyers, Michael P., Paul DeMott, and W. C.: New Primary Ice-Nucleation Parameterizations in an Explicit Cloud Model, J.
935 Appl. Meteorol. Climatol., 1992.

Mihalopoulos, N., Stephanou, E., Kanakidou, M., Pilitsidis, S., and Bousquet, P.: Tropospheric aerosol ionic composition in the Eastern Mediterranean region, Tellus, Ser. B Chem. Phys. Meteorol., 49B, 314–326, https://doi.org/10.3402/tellusb.v49i3.15970, 1997.

Miller, R. L., Knippertz, P., Pérez García-Pando, C., Perlwitz, J. P., and Tegen, I.: Impact of dust radiative forcing upon
940 climate, in: Mineral Dust: A Key Player in the Earth System, Springer Netherlands, Dordrecht, 327–357, https://doi.org/10.1007/978-94-017-8978-3_13, 2014.

Morales Betancourt, R., Lee, D., Oreopoulos, L., Sud, Y. C., Barahona, D., and Nenes, A.: Sensitivity of cirrus and mixed-phase clouds to the ice nuclei spectra in McRAS-AC: Single column model simulations, Atmos. Chem. Phys., 12, 10679–10692, https://doi.org/10.5194/acp-12-10679-2012, 2012.

945 Murray, B. J., O'Sullivan, D., Atkinson, J. D., and Webb, M. E.: Ice nucleation by particles immersed in supercooled cloud droplets., Chem. Soc. Rev., 41, 6519–54, https://doi.org/10.1039/c2cs35200a, 2012.

Myriokefalitakis, S., Tsigaridis, K., Mihalopoulos, N., Sciare, J., Nenes, A., Kawamura, K., Segers, A., and Kanakidou, M.: In-cloud oxalate formation in the global troposphere: A 3-D modeling study, Atmos. Chem. Phys., 11, 5761–5782, https://doi.org/10.5194/acp-11-5761-2011, 2011.

950 Myriokefalitakis, S., Daskalakis, N., Mihalopoulos, N., Baker, A. R., Nenes, A., and Kanakidou, M.: Changes in dissolved iron deposition to the oceans driven by human activity: a 3-D global modelling study, 12, 3973–3992, https://doi.org/10.5194/bg-12-3973-2015, 2015.

Myriokefalitakis, S., Nenes, A., Baker, A. R., Mihalopoulos, N., and Kanakidou, M.: Bioavailable atmospheric phosphorous supply to the global ocean: A 3-D global modeling study, 13, 6519–6543, https://doi.org/10.5194/bg-13-6519-2016, 2016.

955 Myriokefalitakis, S., Daskalakis, N., Kalivitis, N., Chatziparaschos, M., Myriokefalitakis, S., Daskalakis, N., Myriokefalitakis, S., Fanourgakis, G., Origin, M., and Presentation, P.: Arios hatziparaschos, 23–24, 2021.

Van Noije, T. P. C., Le Sager, P., Segers, A. J., Van Velthoven, P. F. J., Krol, M. C., Hazeleger, W., Williams, A. G., and Chambers, S. D.: Simulation of tropospheric chemistry and aerosols with the climate model EC-Earth, Geosci. Model Dev.,

15

965 7, 2435–2475, https://doi.org/10.5194/gmd-7-2435-2014, 2014.

O'Sullivan, D., Murray, B. J., Malkin, T. L., Whale, T. F., Umo, N. S., Atkinson, J. D., Price, H. C., Baustian, K. J., Browse, J., and Webb, M. E.: Ice nucleation by fertile soil dusts: Relative importance of mineral and biogenic components, Atmos. Chem. Phys., 14, 1853–1867, https://doi.org/10.5194/acp-14-1853-2014, 2014.

O'Sullivan, D., Murray, B. J., Ross, J. F., and Webb, M. E.: The adsorption of fungal ice-nucleating proteins on mineral dusts:
970 a terrestrial reservoir of atmospheric ice-nucleating particles, Atmos. Chem. Phys., 16, 7879–7887, https://doi.org/10.5194/acp-16-7879-2016, 2016.

O'Sullivan, D., Adams, M. P., Tarn, M. D., Harrison, A. D., Vergara-Temprado, J., Porter, G. C. E., Holden, M. A., Sanchez-Marroquin, A., Carotenuto, F., Whale, T. F., McQuaid, J. B., Walshaw, R., Hedges, D. H. P., Burke, I. T., Cui, Z., and Murray, B. J.: Contributions of biogenic material to the atmospheric ice-nucleating particle population in North Western Europe, Sci.
975 Rep., 8, 1–9, https://doi.org/10.1038/s41598-018-31981-7, 2018.

Pérez García-Pando, C., Miller, R. L., Perlwitz, J. P., Rodríguez, S., and Prospero, J. M.: Predicting the mineral composition of dust aerosols: Insights from elemental composition measured at the Izaï¿½a Observatory, Geophys. Res. Lett., 43, 10,520-10,529, https://doi.org/10.1002/2016GL069873, 2016.

Perlwitz, J. P., Pérez García-Pando, C., and Miller, R. L.: Predicting the mineral composition of dust aerosols – Part 1:
980 Representing key processes, Atmos. Chem. Phys., 15, 11593–11627, https://doi.org/10.5194/acp-15-11593-2015, 2015a.

Perlwitz, J. P., Pérez García-Pando, C., and Miller, R. L.: Predicting the mineral composition of dust aerosols – Part 2: Model evaluation and identification of key processes with observations, Atmos. Chem. Phys., 15, 11629–11652, https://doi.org/10.5194/acp-15-11629-2015, 2015b.

Pikridas, M., Vrekoussis, M., Sciare, J., Kleanthous, S., Vasiliadou, E., Kizas, C., Savvides, C., and Mihalopoulos, N.: Spatial
985 and temporal (short and long-term) variability of submicron, fine and sub-10 Mm particulate matter (PM1, PM2.5, PM10) in Cyprus, Atmos. Environ., 191, 79–93, https://doi.org/10.1016/j.atmosenv.2018.07.048, 2018.

Pratt, K. a., DeMott, P. J., French, J. R., Wang, Z., Westphal, D. L., Heymsfield, A. J., Twohy, C. H., Prenni, A. J., and Prather, K. a.: In situ detection of biological particles in cloud ice-crystals, Nat. Geosci., 2, 398–401, https://doi.org/10.1038/ngeo521, 2009.

990 Price, H. C., Baustian, K. J., McQuaid, J. B., Blyth, A., Bower, K. N., Choularton, T., Cotton, R. J., Cui, Z., Field, P. R., Gallagher, M., Hawker, R., Merrington, A., Miltenberger, A., Neely, R. R., Parker, S. T., Rosenberg, P. D., Taylor, J. W., Trembath, J., Vergara-Temprado, J., Whale, T. F., Wilson, T. W., Young, G., and Murray, B. J.: Atmospheric Ice-Nucleating Particles in the Dusty Tropical Atlantic, J. Geophys. Res. Atmos., 123, 2175–2193, https://doi.org/10.1002/2017JD027560, 2018.

995 Prospero, J. M., Barkley, A. E., Gaston, C. J., Gatineau, A., Campos y Sansano, A., and Panechou, K.: Characterizing and Quantifying African Dust Transport and Deposition to South America: Implications for the Phosphorus Budget in the Amazon Basin, Global Biogeochem. Cycles, 34, 1–24, https://doi.org/10.1029/2020GB006536, 2020.

Pruppacher, H. R., Klett, J. D., and K., W. P.: Microphysics of Clouds and Precipitation, Aerosol Sci. Technol., 28, 381–382, https://doi.org/10.1080/02786829808965531, 1998a.

1000 Pruppacher, H. R., Klett, J. D., and Wang, P. K.: Microphysics of Clouds and Precipitation, Aerosol Sci. Technol., 28, 381–382, https://doi.org/10.1080/02786829808965531, 1998b.

Roberts, P. and Hallett, J.: A laboratory study of the ice nucleating properties of some mineral particulates, Q. J. R. Meteorol. Soc., 95, 204–205, https://doi.org/10.1002/qj.49709540317, 1969.

Rosenfeld, D., Lohmann, U., Raga, G. B., O'Dowd, C. D., Kulmala, M., Fuzzi, S., Reissell, A., and Andreae, M. O.: Flood or
1005 drought: How do aerosols affect precipitation?, Science (80-.)., 321, 1309–1313, https://doi.org/10.1126/science.1160606, 2008.

Seinfeld, J. H., Bretherton, C., Carslaw, K. S., Coe, H., DeMott, P. J., Dunlea, E. J., Feingold, G., Ghan, S., Guenther, A. B.,

16

Deleted: 2015

Kahn, R., Kraucunas, I., Kreidenweis, S. M., Molina, M. J., Nenes, A., Penner, J. E., Prather, K. A., Ramanathan, V.,
Ramaswamy, V., Rasch, P. J., Ravishankara, A. R., Rosenfeld, D., Stephens, G., and Wood, R.: Improving our fundamental
understanding of the role of aerosol-cloud interactions in the climate system, Proc. Natl. Acad. Sci. U. S. A., 113, 5781–5790,
https://doi.org/10.1073/pnas.1514043113, 2016.

Senthil Kumar, R. and Rajkumar, P.: Characterization of minerals in air dust particles in the state of Tamilnadu, India through
ftir spectroscopy, Atmos. Chem. Phys. Discuss., 13, 22221–22248, https://doi.org/10.5194/acpd-13-22221-2013, 2013.

Si, M., Evoy, E., Yun, J., Xi, Y., Hanna, S. J., Chivulescu, A., Rawlings, K., Veber, D., Platt, A., Kunkel, D., Hoor, P., Sharma,
S., Richard Leaitch, W., and Bertram, A. K.: Concentrations, composition, and sources of ice-nucleating particles in the
Canadian High Arctic during spring 2016, Atmos. Chem. Phys., 19, 3007–3024, https://doi.org/10.5194/acp-19-3007-2019,
2019.

Solomon, A., De Boer, G., Creamean, J. M., McComiskey, A., Shupe, M. D., Maahn, M., and Cox, C.: The relative impact of
cloud condensation nuclei and ice nucleating particle concentrations on phase partitioning in Arctic mixed-phase stratocumulus
clouds, Atmos. Chem. Phys., 18, 17047–17059, https://doi.org/10.5194/acp-18-17047-2018, 2018.

Sotiropoulou, G., Sullivan, S., Savre, J., Lloyd, G., Lachlan-Cope, T., Ekman, A. M. L., and Nenes, A.: The impact of
secondary ice production on Arctic stratocumulus, Atmos. Chem. Phys., 20, 1301–1316, https://doi.org/10.5194/acp-20-1301-
2020, 2020.

Sotiropoulou, G., Vignon, E., Young, G., Morrison, H., O'Shea, S. J., Lachlan-Cope, T., Berne, A., and Nenes, A.: Secondary
ice production in summer clouds over the Antarctic coast: An underappreciated process in atmospheric models, Atmos. Chem.
Phys., 21, 755–771, https://doi.org/10.5194/acp-21-755-2021, 2021.

Spracklen, D. V. and Heald, C. L.: The contribution of fungal spores and bacteria to regional and global aerosol number and
ice nucleation immersion freezing rates, Atmos. Chem. Phys., 14, 9051–9059, https://doi.org/10.5194/acp-14-9051-2014,
2014.

Sullivan, S. C., Hoose, C., Kiselev, A., Leisner, T., and Nenes, A.: Initiation of secondary ice production in clouds, Atmos.
Chem. Phys., 18, 1593–1610, https://doi.org/10.5194/acp-18-1593-2018, 2018.

Tegen, I., Harrison, S. P., Kohfeld, K., Prentice, I. C., Coe, M., and Heimann, M.: Impact of vegetation and preferential source
areas on global dust aerosol: Results from a model study, J. Geophys. Res. Atmos., 107,
https://doi.org/10.1029/2001JD000963, 2002.

Tsigaridis, K. and Kanakidou, M.: Secondary organic aerosol importance in the future atmosphere, Atmos. Environ., 41, 4682–
4692, https://doi.org/10.1016/j.atmosenv.2007.03.045, 2007.

Tsigaridis, K., Krol, M., Dentener, F. J., Balkanski, Y., Lathière, J., Metzger, S., Hauglustaine, D. A., and Kanakidou, M.:
Change in global aerosol composition since preindustrial times, Atmos. Chem. Phys., 6, 5143–5162,
https://doi.org/10.5194/acp-6-5143-2006, 2006.

Tsigaridis, K., Daskalakis, N., Kanakidou, M., Adams, P. J., Artaxo, P., Bahadur, R., Balkanski, Y., Bauer, S. E., Bellouin,
N., Benedetti, A., Bergman, T., Berntsen, T. K., Beukes, J. P., Bian, H., Carslaw, K. S., Chin, M., Curci, G., Diehl, T., Easter,
R. C., Ghan, S. J., Gong, S. L., Hodzic, A., Hoyle, C. R., Iversen, T., Jathar, S., Jimenez, J. L., Kaiser, J. W., Kirkeväg, A.,
Koch, D., Kokkola, H., H Lee, Y., Lin, G., Liu, X., Luo, G., Ma, X., Mann, G. W., Mihalopoulos, N., Morcrette, J. J., Müller,
J. F., Myhre, G., Myriokefalitakis, S., Ng, N. L., O'donnell, D., Penner, J. E., Pozzoli, L., Pringle, K. J., Russell, L. M., Schulz,
M., Sciare, J., Seland, Shindell, D. T., Sillman, S., Skeie, R. B., Spracklen, D., Stavrakou, T., Steenrod, S. D., Takemura, T.,
Tiitta, P., Tilmes, S., Tost, H., Van Noije, T., Van Zyl, P. G., Von Salzen, K., Yu, F., Wang, Z., Wang, Z., Zaveri, R. A.,
Zhang, H., Zhang, K., Zhang, Q., and Zhang, X.: The AeroCom evaluation and intercomparison of organic aerosol in global
models, Atmos. Chem. Phys., 14, 10845–10895, https://doi.org/10.5194/acp-14-10845-2014, 2014.

Vali, G., DeMott, P. J., Möhler, O., and Whale, T. F.: Technical Note: A proposal for ice nucleation terminology, Atmos.
Chem. Phys., 15, 10263–10270, https://doi.org/10.5194/acp-15-10263-2015, 2015.

Vergara-Temprado, J., Murray, B. J., Wilson, T. W., O'Sullivan, D., Browse, J., Pringle, K. J., Ardon-Dryer, K., Bertram, A. K., Burrows, S. M., Ceburnis, D., Demott, P. J., Mason, R. H., O'Dowd, C. D., Rinaldi, M., and Carslaw, K. S.: Contribution of feldspar and marine organic aerosols to global ice nucleating particle concentrations, Atmos. Chem. Phys., 17, 3637–3658, https://doi.org/10.5194/acp-17-3637-2017, 2017.

Vergara-Temprado, J., Miltenberger, A. K., Furtado, K., Grosvenor, D. P., Shipway, B. J., Hill, A. A., Wilkinson, J. M., Field, P. R., Murray, B. J., and Carslaw, K. S.: Strong control of Southern Ocean cloud reflectivity by ice-nucleating particles, Proc. Natl. Acad. Sci. U. S. A., 115, 2687–2692, https://doi.org/10.1073/pnas.1721627115, 2018.

Violaki, K., Nenes, A., Tsagkaraki, M., Paglione, M., Jacquet, S., Sempéré, R., and Panagiotopoulos, C.: Bioaerosols and dust are the dominant sources of organic P in atmospheric particles, npj Clim. Atmos. Sci., 4, https://doi.org/10.1038/s41612-021-00215-5, 2021.

Wang, Y., Liu, X., Hoose, C., and Wang, B.: Different contact angle distributions for heterogeneous ice nucleation in the community atmospheric model version 5, Atmos. Chem. Phys., 14, 10411–10430, https://doi.org/10.5194/acp-14-10411-2014, 2014.

Wex, H., Huang, L., Zhang, W., Hung, H., Traversi, R., Becagli, S., Sheesley, R. J., Moffett, C. E., Barrett, T. E., Bossi, R., Skov, H., Hünerbein, A., Lubitz, J., Löffler, M., Linke, O., Hartmann, M., Herenz, P., and Stratmann, F.: Annual variability of ice-nucleating particle concentrations at different Arctic locations, Atmos. Chem. Phys., 19, 5293–5311, https://doi.org/10.5194/acp-19-5293-2019, 2019.

Whale, T. F., Holden, M. A., Wilson, T. W., O'Sullivan, D., and Murray, B. J.: The enhancement and suppression of immersion mode heterogeneous ice-nucleation by solutes, Chem. Sci., 9, 4142–4151, https://doi.org/10.1039/c7sc05421a, 2018.

Wilson, T. W., Ladino, L. A., Alpert, P. A., Breckels, M. N., Brooks, I. M., Browse, J., Burrows, S. M., Carslaw, K. S., Huffman, J. A., Judd, C., Kilthau, W. P., Mason, R. H., McFiggans, G., Miller, L. A., Nájera, J. J., Polishchuk, E., Rae, S., Schiller, C. L., Si, M., Temprado, J. V., Whale, T. F., Wong, J. P. S., Wurl, O., Yakobi-Hancock, J. D., Abbatt, J. P. D., Aller, J. Y., Bertram, A. K., Knopf, D. A., and Murray, B. J.: A marine biogenic source of atmospheric ice-nucleating particles, Nature, 525, 234–238, https://doi.org/10.1038/nature14986, 2015.

Yin, J., Wang, D., and Guoqing, Z.: An Evaluation of Ice Nuclei Characteristics from the Long-term Measurement Data over North China An Evaluation of Ice Nuclei Characteristics from the Long-term Measurement Data over North China, https://doi.org/10.1007/s13143-012-0020-8, 2012.

Zuidema, P., Alvarez, C., Kramer, S. J., Custals, L., Izaguirre, M., Sealy, P., Prospero, J. M., and Blades, E.: Is summer African dust arriving earlier to Barbados?, Bull. Am. Meteorol. Soc., 100, 1981–1986, https://doi.org/10.1175/BAMS-D-18-0083.1, 2019.
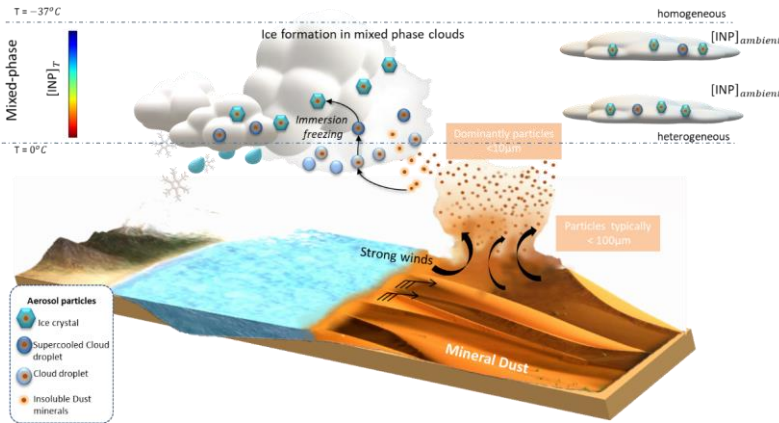
Figure 1: Illustration of the formation of INP from mineral dust aerosol and the two ways in which we display INP concentrations in the present study: [INP]ambient calculated at ambient model temperature relevant to non-deep convective mixed-phase clouds using the ambient temperature in the model temperature level (right part of the figure), and [INP]T calculated at a fixed temperature relevant for vertically extended clouds as deep-convective systems (left part of the figure). The temperature color scale from 0 to -37oC is provided to the left (see text). Figure modified by combining the ones in Kanji et al. 2017 (Figure 1), Harrison et al. 2019 (Figure 1) and Vergara-Temprado et al. 2017 (Figure 3).
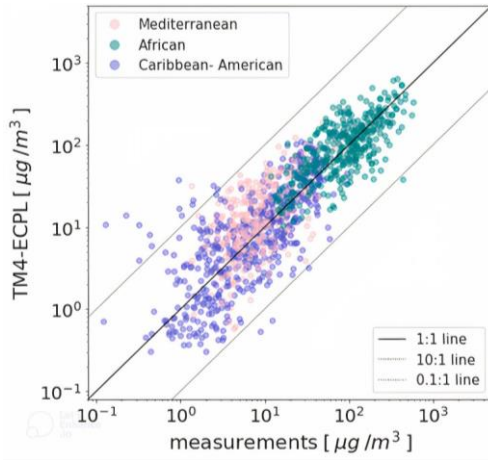
Figure 2: Monthly averaged model-simulated versus observed dust concentration at the selected locations in µg·m⁻³. The continuous black line is the 1:1 line, while the dashed lines are the 10:1 and 1:10, top and bottom lines, respectively. The stations are geographically grouped: African stations in green (M'bour, Bambey, Cinzana, Banizoumbou), American stations in violet (Miami, Barbados, Cayenne), and Mediterranean stations in pink (Agia Marina and Finokalia). Simulations were run with a 3°x2° spatial resolution.
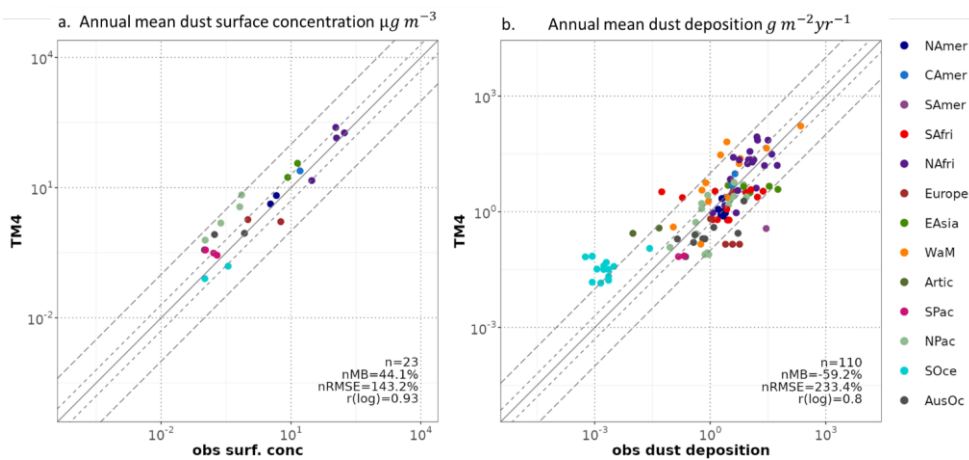
19

Figure 3: Comparison of (a) the modelled annual mean dust surface concentration for the years 2009–2016 compared to climatological mean values from RSMAS sites and AMMA campaign, and (b) comparison of modelled annual dust deposition flux averaged for the same period against observations compiled in Albani et al. (2014) from several sources. The solid line represents the 1 : 1 correspondence, the long dashed lines show the 10 : 1 and 1 : 10 relationships and short dashed lines corresponds to a factor of 2, respectively. Colors indicate measurement locations listed in the figure legend.
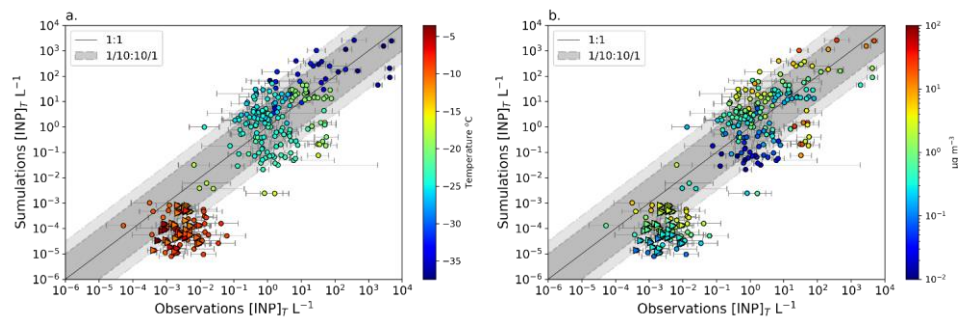
Figure 4: Comparison of [INP]$_T$ concentrations calculated at the temperature of the measurements against observations (dates and locations provided in the supplementary Table S1). For each observation, the INP concentration is calculated at the temperature corresponding to the instrument temperature of the measurement. Circle markers correspond to the BACCHUS database and triangles to Wex et al. (2019) database. The dark grey dashed lines represent one order of magnitude of difference between modelled and observed, and the light-grey dashed lines 1.5 orders of magnitude. The simulated values correspond to monthly mean concentration, and the error bars correspond to the observed error of monthly mean INP values. The color bars show the corresponding instrument temperature of the measurement in Celsius (a) and the modelled dust aerosol mass concentration in μg m^{-3} (b).
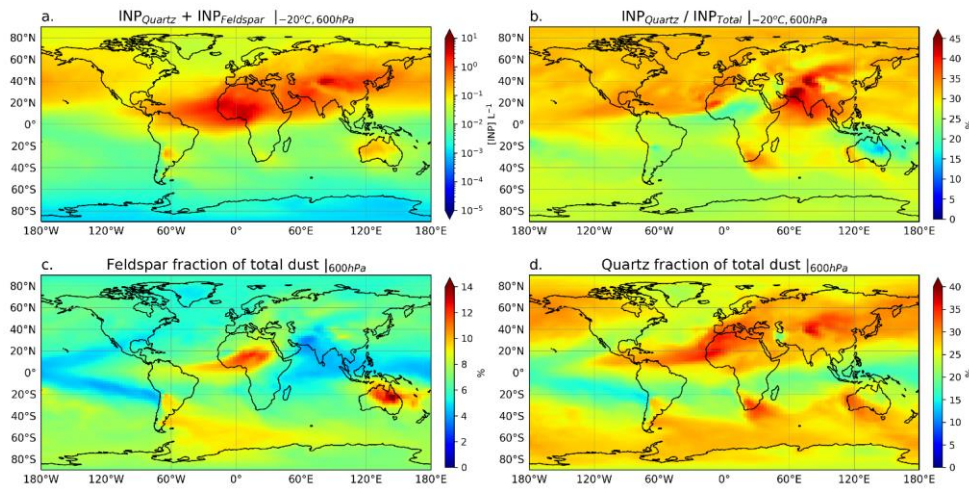
Figure 5: Annual mean distributions calculated by TM4-ECPL for the year 2015 of (a) INP concentrations for an activation temperature of −20oC based on K-feldspar and quartz at a pressure level of 600 hPa, (b) ratio of INP from quartz over total INPs from dust (K-feldspar and quartz) at the same conditions, (c and d) mass ratios of feldspar (c) and quartz (d) in percentages over total dust mass at 600hPa.
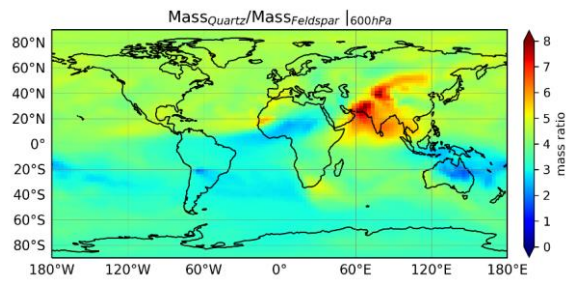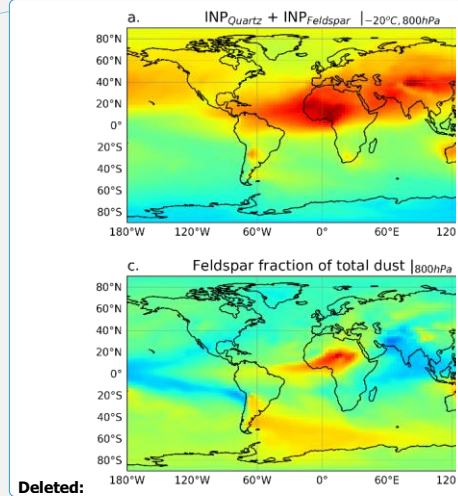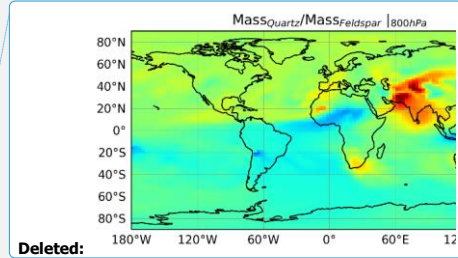
Figure 6: Ratio of quartz to feldspar minerals masses in dust as calculated by dividing quartz mass by feldspar mass.

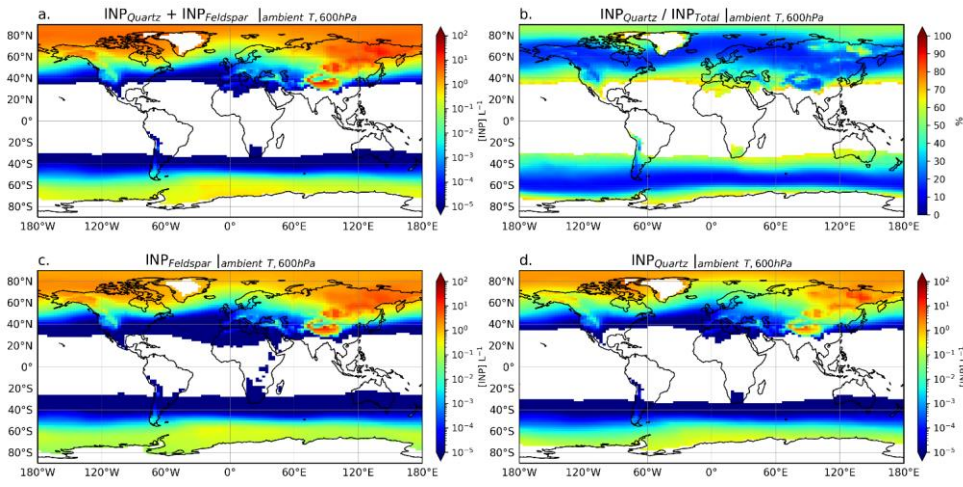**Figure 7: Annual mean distributions of ice-nucleating particles number concentrations [INP]ambient calculated by TM4-ECPL at ambient (model's) temperature and 600 hPa based on the presence both of K-feldspar and quartz (a). Ratio of INP from quartz over total INP from K-feldspar and quartz at the same conditions (b). Panels (c-d) show the corresponding INP concentrations derived individually from each mineral: K-feldspar (c) and quartz (d).**
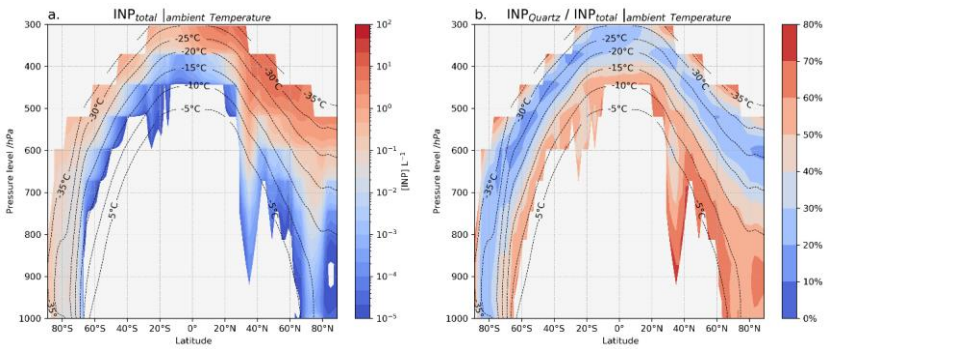
Figure 8: Annual zonal mean profiles of [INP]ambient number concentration for 2015, calculated by TM4-ECPL and accounting for K-feldspar and quartz. The black contour dashed lines show the annual mean temperature of the model. The color map shows the INP concentration derived from feldspar and quartz dust aerosols [INP]total (a) and the ratio of INP from quartz to the total INP from both minerals (b).